AGU PUBLICATIONS

Water Resources Research

RESEARCH ARTICLE

10.1002/2015WR018547

Key Points:

- A novel statistical-dynamical drought prediction model
- Combines a physically based approach with an analog-year concept
- Model improves drought prediction in southwestern United States

Correspondence to:
A. AghaKouchak,
amir.a@uci.edu

Citation:
Madadgar, S., A. AghaKouchak, S. Shukla, A. W. Wood, L. Cheng, K.-L. Hsu, and M. Svoboda (2016), A hybrid statistical-dynamical framework for meteorological drought prediction: Application to the southwestern United States, *Water Resour. Res.*, *52*, 5095–5110, doi:10.1002/2015WR018547.

Received 22 DEC 2015
Accepted 2 JUN 2016
Accepted article online 6 JUN 2016
Published online 2 JUL 2016

A hybrid statistical-dynamical framework for meteorological drought prediction: Application to the southwestern United States

Shahrbanou Madadgar[1], Amir AghaKouchak[1], Shraddhanand Shukla[2], Andrew W. Wood[3], Linyin Cheng[4], Kou-Lin Hsu[1], and Mark Svoboda[5]

[1]Department of Civil and Environmental Engineering, University of California, Irvine, California, USA, [2]Department of Geography, University of California, Santa Barbara, California, USA, [3]Research Applications Laboratory, National Center for Atmospheric Research, Boulder, Colorado, USA, [4]Cooperative Institute for Research in Environmental Sciences, University of Colorado Boulder, Boulder, Colorado, USA, [5]National Drought Mitigation Center, University of Nebraska-Lincoln, Lincoln, Nebraska, USA

Abstract Improving water management in water stressed-regions requires reliable seasonal precipitation predication, which remains a grand challenge. Numerous statistical and dynamical model simulations have been developed for predicting precipitation. However, both types of models offer limited seasonal predictability. This study outlines a hybrid statistical-dynamical modeling framework for predicting seasonal precipitation. The dynamical component relies on the physically based North American Multi-Model Ensemble (NMME) model simulations (99 ensemble members). The statistical component relies on a multivariate Bayesian-based model that relates precipitation to atmosphere-ocean teleconnections (also known as an analog-year statistical model). Here the Pacific Decadal Oscillation (PDO), Multivariate ENSO Index (MEI), and Atlantic Multidecadal Oscillation (AMO) are used in the statistical component. The dynamical and statistical predictions are linked using the so-called Expert Advice algorithm, which offers an ensemble response (as an alternative to the ensemble mean). The latter part leads to the best precipitation prediction based on contributing statistical and dynamical ensembles. It combines the strength of physically based dynamical simulations and the capability of an analog-year model. An application of the framework in the southwestern United States, which has suffered from major droughts over the past decade, improves seasonal precipitation predictions (3–5 month lead time) by 5–60% relative to the NMME simulations. Overall, the hybrid framework performs better in predicting negative precipitation anomalies (10–60% improvement over NMME) than positive precipitation anomalies (5–25% improvement over NMME). The results indicate that the framework would likely improve our ability to predict droughts such as the 2012–2014 event in the western United States that resulted in significant socioeconomic impacts.

1. Introduction

Water supply reliability is a major challenge in the southwestern United States (U.S.), with its growing population and industry. The region has experienced several droughts in the past [*Seager et al.*, 2005; *Woodhouse et al.*, 2010; *Shukla et al.*, 2015a, 2015b; *Cheng et al.*, 2016] and is likely to experience more frequent and severe droughts in the future [*Seager et al.*, 2007; *Cayan et al.*, 2010; *Cook et al.*, 2015]. The water supply in some parts of the region (e.g., California and Nevada) relies on winter precipitation, when most of the annual rainfall occurs [*Cayan et al.*, 1998]. The ongoing 2012–2015 California drought has led to more than a year's worth of precipitation deficit [*Savtchenko et al.*, 2015]. The rainy seasons in 2014 and 2015 were also the warmest 2 years in the past 120 years [*Shukla et al.*, 2015b; *AghaKouchak et al.*, 2014]. Such combinations of below-normal precipitation and high temperature can significantly exacerbate the impacts of drought by promoting wildfires [*Westerling et al.*, 2003; *Keeley et al.*, 2009] and reducing snowpack in high elevations [*Shukla et al.*, 2015b].

The sustainable management of water resources in a region with frequent droughts requires timely and reliable seasonal precipitation forecasts. A community report on California drought issues that was developed based on inputs from decision-makers and stakeholders identified seasonal drought prediction as the key challenge facing the research community [*AghaKouchak et al*., 2015]. The observed relationship between precipitation and the ocean-atmosphere teleconnections [*Ropelewski and Halpert*, 1986; *Bradley et al*., 1987; McCabe and *Dettinger*, 1999] has inspired the investigation and use of statistical analog-year models for seasonal precipitation forecasting [e.g., *Hartmann et al*., 2008; *Wu et al*., 2009; *Schepen et al*., 2012; *Peng et al*., 2014]. Many alternatives of analog-year precipitation prediction methods have been explored [e.g., *Saha et al*., 2014; *Zhang et al*., 2007]. Although such models display some prediction skills, their predictability is limited due to the complex relationship between precipitation and the known teleconnections [e.g., *Folland et al*., 1991; *Gershunov*, 1998; *Obled et al*., 2002; *Rajeevan et al*., 2007].

Physically based dynamical models have also been explored for seasonal precipitation prediction. Unlike statistical techniques, these models rely on the dynamical interactions among the land, ocean, and atmosphere, which are resolved using model parameterization and numerical simulations [e.g., *Zhang et al*., 2007; *Merryfield et al*., 2013; *Saha et al*., 2014]. Progress in dynamical model simulations over the past three decades has led to better and more reliable predictions. However, the predictability of dynamical model simulations is still rather limited and is highly variable in space and time [*Yang et al*., 2009; *Wang et al*., 2009; *Kim et al*., 2012; *Infanti and Kirtman*, 2015; *Jia et al*., 2015]. Previous studies have shown that the forecasting skill of dynamical models is mainly explained by the El Nino-Southern Oscillation (ENSO) variability [*Kumar et al*., 2007; *Wang et al*., 2009; *Cohen and Jones*, 2011], which itself does not fully account for the total variability in precipitation [*Gao et al*., 2006]. To overcome, the limitations of individual dynamical models and benefit from the strength of a diverse set of models, there has been a growing tendency to use multiple models and combine their forecasts [*Hewitt*, 2004; *Palmer et al*., 2004; *Bougeault et al*., 2010]. Recently, a multiagency effort led to the development of the North American Multi-Model Ensemble (NMME) [*Kirtman et al*., 2014], which has provided climate forecasts ranging from intra-seasonal to inter-seasonal scales. The NMME ensemble average generally offers better predictions than individual contributing models do for different regions [*Becker et al*., 2014; *Kirtman et al*., 2014; *Ma et al*., 2015]; however, the reliability of the precipitation forecasts in general is still rather low [*Becker et al*., 2014; *Kirtman et al*., 2014]. As an example, Figure 1 shows the observed and NMME-predicted anomalies for December 2014 to February 2015 precipitation (DJF 2014), from a forecast initial condition in October 2014. As shown, the NMME's precipitation prediction for DJF 2014 was not consistent with the observations in the western U.S. (i.e., the NMME indicated a positive precipitation anomaly, but the region experienced one of its most extreme droughts). Similar maps based on different initialization dates can be found through Climate Prediction Center (http://www.cpc.ncep.noaa.gov/products/NMME/http://www.cpc.ncep.noaa.gov/products/NMME/).

Previous studies have argued that combining statistical and dynamical models can improve seasonal precipitation prediction [*Coelho et al*., 2004; *Schepen et al*., 2012]. This study outlines a hybrid framework for combining dynamical and statistical seasonal precipitation forecasts to improve their skill, with consequent benefits for improved drought prediction in the southwest U.S. and other regions. The proposed hybrid framework is fundamentally different from the statistical postprocessing approaches in which a statistical model is used to combine multiple dynamical models, e.g., by weighing the ensemble members [*Raftery et al*., 2005; *Luo et al*., 2007; *Schepen and Wang*, 2013]. It follows instead a hierarchical approach also taken by *Schepen et al*. [2014], where dynamical and statistical models work in parallel and offer their own predictions, and are subsequently merged into a single prediction. Here the dynamical component is based on the available NMME simulations. The statistical forecasts employ a Bayesian analog-year approach that simulates precipitation based on a number of conditioning factors, such as the Pacific Decadal Oscillation (PDO), Multivariate ENSO Index (MEI), and Atlantic Multidecadal Oscillation (AMO). The statistical analog-year forecasts and the NMME dynamical model simulations are then combined via a multimodel averaging framework. In contrast to the conventional ensemble mean, the weighted averaging techniques such as Bayesian-based techniques [*Raftery et al*., 2005; *Buser et al*., 2010; *Najafi and Moradkhani*, 2015] and expert-based algorithms [*Cheng and AghaKouchak*, 2015] distribute the weights based on the performance of each model during a training period. The final ensemble response from weighted averaging techniques generally outperforms the single best model [*Weigel et al*., 2008] and the simple ensemble mean, except under particular circumstances such as extremely large variability in models [*Weigel et al*., 2010]. This study uses the so-called Expert Advice (hereafter, EA) algorithm described in *Cheng and AghaKouchak* [2015], which returns the weighted average of the ensemble that is supposedly the best response from the ensemble of statistical and dynamical simulations.

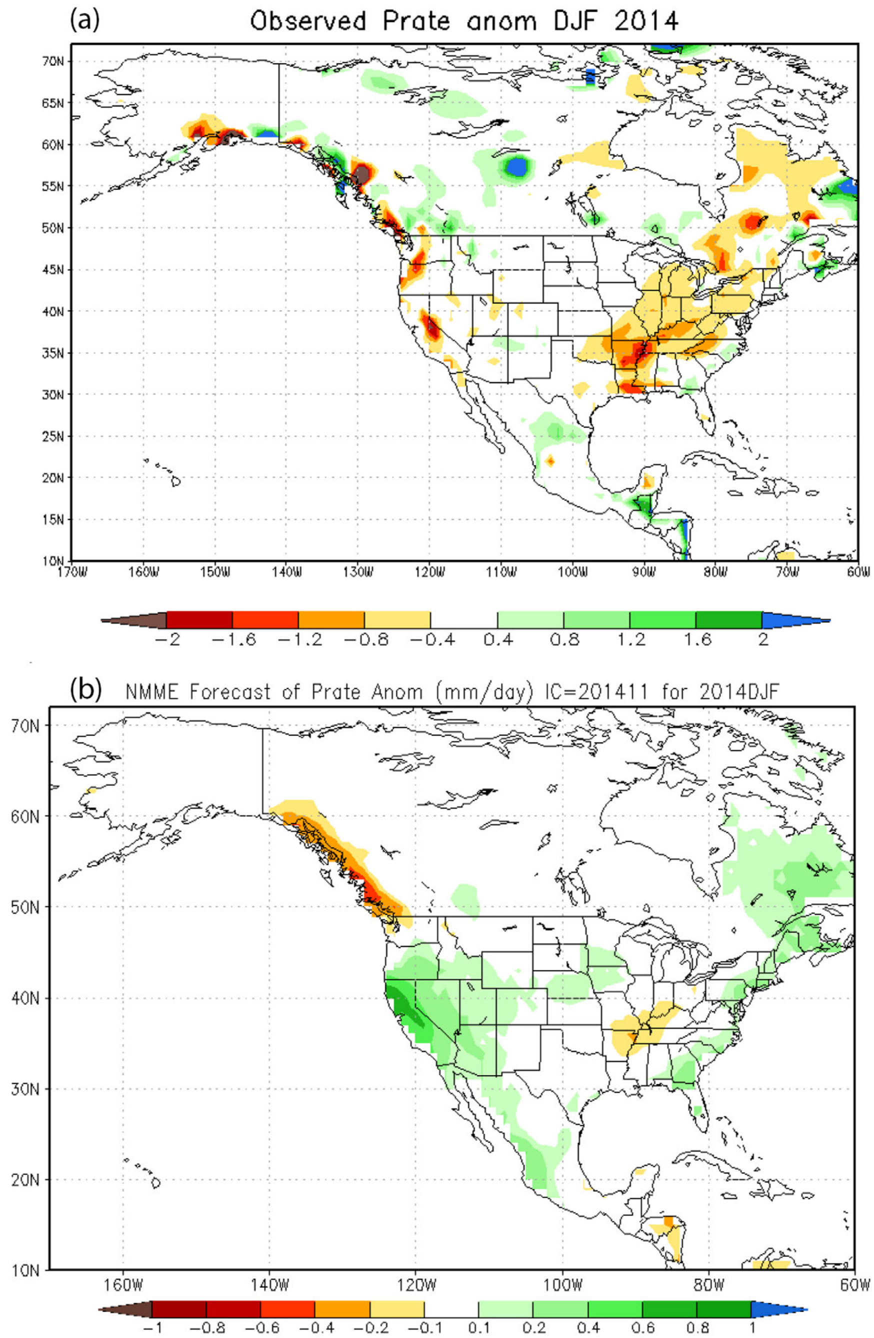

Figure 1. Comparison between (a) the observed precipitation and (b) the NMME simulation for the anomalies of the precipitation rate from December 2014 to February 2015. The forecast initial condition is set to October 2014. Note that the color bars in the maps are not in the same scale.

2. Study Area and Data Resources

This study focuses on seasonal precipitation forecasting in California and Nevada. This region has recently suffered from severe droughts, and reliable forecasts have become crucial for improving water management. In California, 75% of the annual precipitation occurs between November and March (i.e., rainy season), with the half occurring between December and February [*Shukla et al*., 2015a]. Given the strong seasonality of precipitation in the region, water management primarily relies on rainy season precipitation. Thus, this study focuses on precipitation forecasting during the rainy season with different lead times. The forecast periods begin from November, December, and January of each year and continues to March; that is, 3–5 month lead times (i.e., NDJ, NDJF, NDJFM, DJF, DJFM, and JFM). All forecasts are initiated on October.

This study proposes a hybrid method to improve precipitation forecasts by combining predictions based on the dynamical model simulations with statistical predictions that leverage atmosphere-ocean teleconnections with the seasonal precipitation. The dynamical model simulations with different lead times are obtained from the North American Multi-Model Ensemble (NMME) [*Kirtman et al*., 2014]. Retrospective NMME simulations for January 1982 to December 2010 are available at the International Research Institute for Climate and Society (IRI)'s climate data library. Real-time forecasts of NMME are also available since August 2011 except a few models (CMC1-CanCM3 and CMC2-CanCM4), which are available since December 2011. To avoid discrepancies in the number of models form one year to another, we excluded 2011 simulations from our analysis and used the rest of data during 1982–2014 for which all model simulations were available. The observed reference precipitation is based on a gridded station-based data record developed for western U.S. forecasting and verification purposes [*Wood*, 2008; *Tang et al*., 2009].

3. Hybrid Forecast Model

This study proposes a hybrid precipitation prediction framework that combines the dynamical NMME forecasts with statistical simulations in each $1^\circ \times 1^\circ$ grid cell across the study area. The purpose of combining these two types of models is to select the best forecasts from the ensemble of dynamical and statistical predictions. Figure 2 shows an overview of the proposed hybrid precipitation prediction model. The dynamical (Figure 2a) and statistical (Figure 2b) simulations run in parallel; each leads to an ensemble of predictions. Then, the forecast ensembles produced from the dynamical and statistical model simulations are overlaid to form the final ensemble (Figure 2c). Last, the EA algorithm, trained with model performance in the past, finds the best ensemble response from the statistical and dynamical predictions (Figure 2d).

3.1. Dynamical Model Simulations

The North America Multi-Model Ensemble (NMME) [*Kirtman et al*., 2014] is an ensemble of simulations from multiple dynamical models and provides probabilistic forecasts with some information regarding forecast uncertainty. Each dynamical model contributes a certain number of ensemble members. In this study, we picked an ensemble of 99 members from eight models which are used by the Climate Prediction Center (CPC) for the operational forecasts (i.e., CMC1-CanCM3 [10], CMC2-CanCM4 [10], COLA-RSMAS-CCSM4 [10], GFDL-CM2p1-aer04 [10], GFDL-CM2p5-FLOR-A06 [12], GFDL-CM2p5-FLOR-B01 [12], NASA-GMAO-062012 [11], and NCEP-CFSv2 [24]) and used the ensemble mean of each model in the hybrid forecast model that is discussed in following sections. We studied the NMME precipitation forecasts beginning from November (initialized in October) with up to a 5 month lead time (i.e., November–March, NDJFM) during 1982–2014, except the year 2011 since some NMME models' data are not available for 2011. This is the rainy season for the study area.

3.2. Statistical Analog-Year Simulations

Several studies have discussed the impacts of atmosphere-ocean teleconnections on seasonal precipitation patterns [*Rasmusson and Wallace*, 1983; *Ropelewski and Halpert*, 1986; *Bradley et al*., 1987; *McCabe and Dettinger*, 1999; *Kurtzman and Scanlon*, 2007; *DeFlorio et al*., 2013]. The ENSO, which represents the fluctuation of sea surface temperature (SST) and air pressure in the tropical eastern Pacific Ocean, affects regional precipitation levels, across several regions of the globe including North America [*Bradley et al*., 1987; *Redmond and Koch*, 1991; *Diaz and Kiladis*, 1992]. The above-normal SST (warm phase or El Nino) and below-normal SST (cold phase or La Nina) in the tropical Pacific Ocean have different climatic impacts [*Bradley et al*., 1987; *Hoerling et al*., 1997; *Trenberth*, 1984, 1997] with variable significance, depending on the signal's strength [*Kiladis and Diaz*, 1989; *Redmond and Koch*, 1991]. For instance, the above-normal precipitation in southern California is usually associated with El Nino episodes [*Redmond and Koch*, 1991], whereas precipitation over northern California does not show a strong association with either El Nino or La Nina episodes [*McCabe and Dettinger*, 1999]. However, the collective information from ENSO signals and the long-term fluctuations in the North Pacific Ocean-indicated as the Pacific Decadal Oscillation (PDO) can improve the precipitation prediction skill in the western U.S. [*McCabe and Dettinger*, 1999]. In addition, the Atlantic Multidecadal Oscillation (AMO), which reflects the long-term changes in the sea surface temperature of the North Atlantic Ocean, affects precipitation and drought

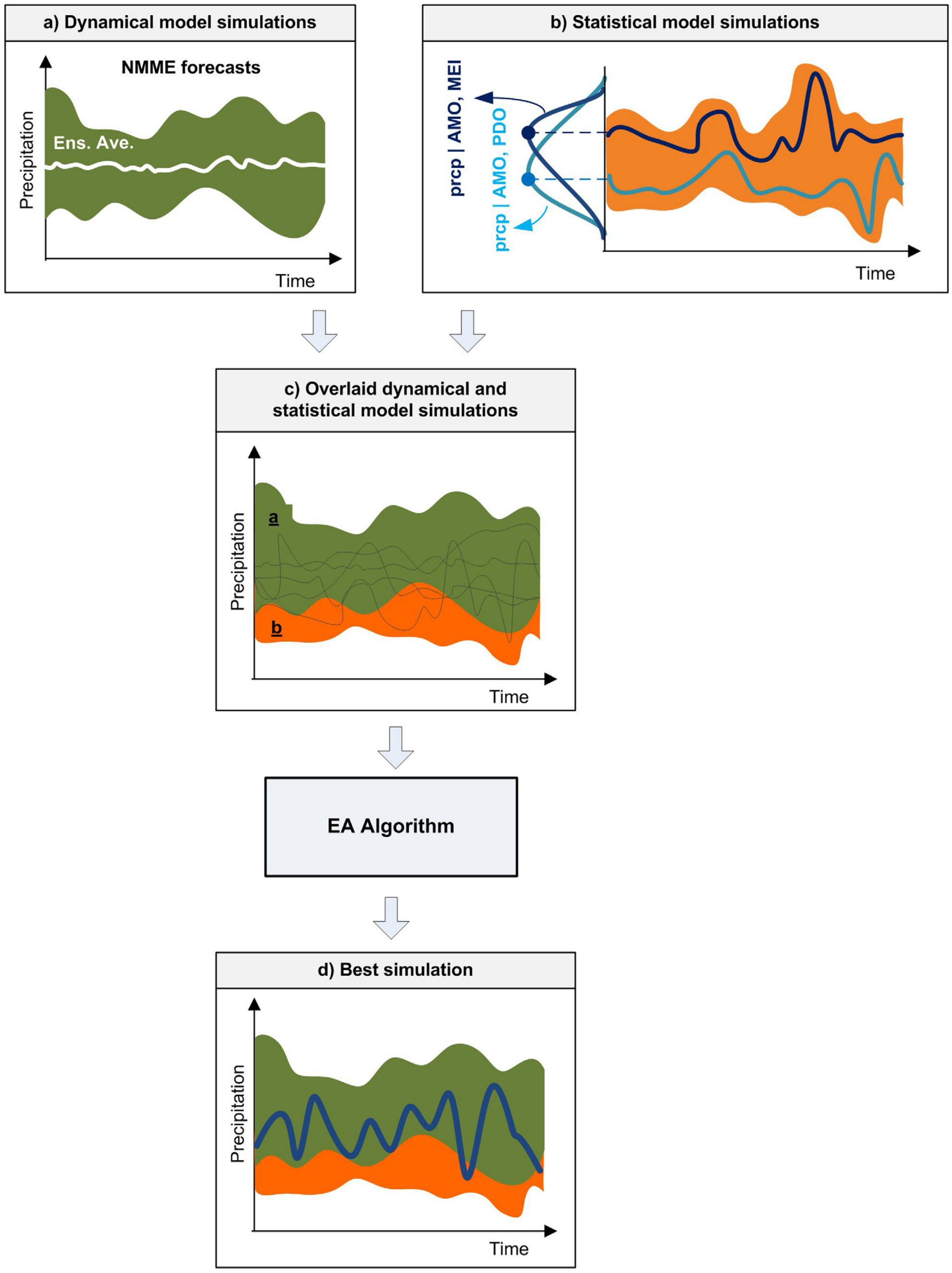

Figure 2. Flowchart of the proposed hybrid statistical-dynamical precipitation forecasting algorithm. See the text for details.

frequency over North America [*McCabe et al*., 2004]. The two major droughts in the twentieth century (1930s and 1950s) occurred during the positive phase of AMO and negative phase of PDO between 1925 and 1965 [*McCabe et al*., 2004]. Given the demonstrated capability of PDO, MEI, and AMO in the prediction of precipitation over North America, this study assesses the potential for these three indices to improve seasonal precipitation forecasts over southwest U.S. The monthly records of teleconnection indices are obtained from the Earth System Research Laboratory at the National Oceanic and Atmospheric Administration (NOAA). More information on PDO, MEI, and AMO and their impacts on the southwestern U.S. is provided in Appendix A.

The proposed hybrid approach benefits from the predictability of an analog-year model based on teleconnection indices [*Hidalgo and Dracup*, 2003; *Kurtzman and Scanlon*, 2007]. We propose a Bayesian model based on copula functions [*Joe*, 1997; *Nelsen*, 1999] to represent the joint distribution of teleconnection indices and seasonal precipitation. Unlike multivariate distribution functions, such as the bivariate Gaussian or Gamma distributions [*Kelly and Krzysztofowicz*, 1997; *Sharma*, 2000; *Yue et al.*, 2001], copulas do not require all of the marginal distributions to come from the same distribution.

Copula functions are defined as multivariate distribution functions, $P(x_1, \ldots, x_n)$, with uniformly distributed variables on the interval $[0, 1]$:

$$P(x_1, \ldots, x_i, \ldots, x_n)=C[P(x_1), \ldots, P(x_i), \ldots, P(x_n)]=C(u_1, \ldots, u_i, \ldots, u_n) \tag{1}$$

where, C is the Cumulative Distribution Function (CDF) of the copula, and $P(x_i)$ is the marginal distribution of x_i being uniform on the interval $[0, 1]$, which is also denoted by u_i. Note that C connects the CDFs of the random variables (i.e., u_i), whereas $P(\ldots)$ in the left-hand side represents the joint probabilities of the original random variables (i.e., x_i).

The Elliptical and Archimedean copulas [*Nelsen*, 1999] are the two families that are most frequently used in hydrologic applications [e.g., *Favre et al.*, 2004; *Dupuis*, 2007; *Hao and AghaKouchak*, 2013; *Madadgar and Moradkhani*, 2015]. Archimedean copulas have limitations in preserving high-dimensional pair-wise dependence [*Joe*, 1997]. Elliptical copulas, on the other hand, are more flexible for describing associations among more than two variables. For this reason, we use Gaussian copula from the elliptical family for the analog-year model as explained below.

We use the conditional probability distribution function based on copulas [*Madadgar and Moradkhani*, 2013] to estimate the predictive distribution of precipitation given the joint status of the teleconnection indices:

$$p(x_1|\ x_2\ \ldots, x_n)=\frac{c(u_1, \ldots, u_n)\prod_{i=1}^{n}p(x_i)}{c(u_2, \ldots, u_n)\prod_{i=2}^{n}p(x_i)} \tag{2}$$

where, $p(x_1|\ x_2\ \ldots, x_n)$ is the conditional distribution of the random variable x_1 given the set $(x_2\ \ldots, x_n)$ of random variables; $c(u_1, \ldots, u_n)$ is the Probability Density Function (PDF) of the continuous copula function; and $p(x_i)$ is the PDF of ith random variable. The conditional probability of x_1 given x_2 (i.e., bivariate case) is expressed as follows:

$$p(x_1|x_2)= c(u_1, u_2).p(x_1) \tag{3}$$

In a trivariate case, the conditional probability of x_1 given x_2, x_3 is defined as

$$p(x_1|x_2, x_3)= \frac{c(u_1, u_2, u_3).p(x_1)}{c(u_2, u_3)} \tag{4}$$

We used equation (4) to estimate the conditional probability of precipitation at each grid cell in the study area (denoted by x_1) given multiple teleconnection indices (denoted by x_2 and x_3) that have been observed in the preceding months/seasons. We have used multiple variables, including PDO, MEI, and AMO, and linked them to precipitation using Gaussian copula as mentioned above. The copula parameters have been estimated using the method of Inference Function for Margins (IFM) [*Joe*, 1997]. The predictive distribution of equation (4) is then obtained once using AMO (i.e., x_2) and MEI (i.e., x_3) and once using AMO (i.e., x_2) and PDO (i.e., x_3). Then, the fiftieth percentiles (median) of the resulting probability distributions are used as the final forecasts; that is, two forecasts each obtained from a separate probability distribution.

3.3. Expert Advice (EA) Algorithm

In the hybrid model, the Expert Advice (EA) algorithm [*Cheng and AghaKouchak*, 2015] is used to combine the dynamical and analog-year statistical components (Figure 2). In this application, the final ensemble in the hybrid model consists of the two statistical analog-year model predictions, the grand ensemble mean of the NMME forecasts, and the ensemble mean of each participating model in the NMME, that is, eight ensemble members from eight models—making a total of eleven inputs to the EA algorithm. The EA algorithm assigns different weights to the ensemble members based on their performance during a training period, and returns their weighted average as the best ensemble response.

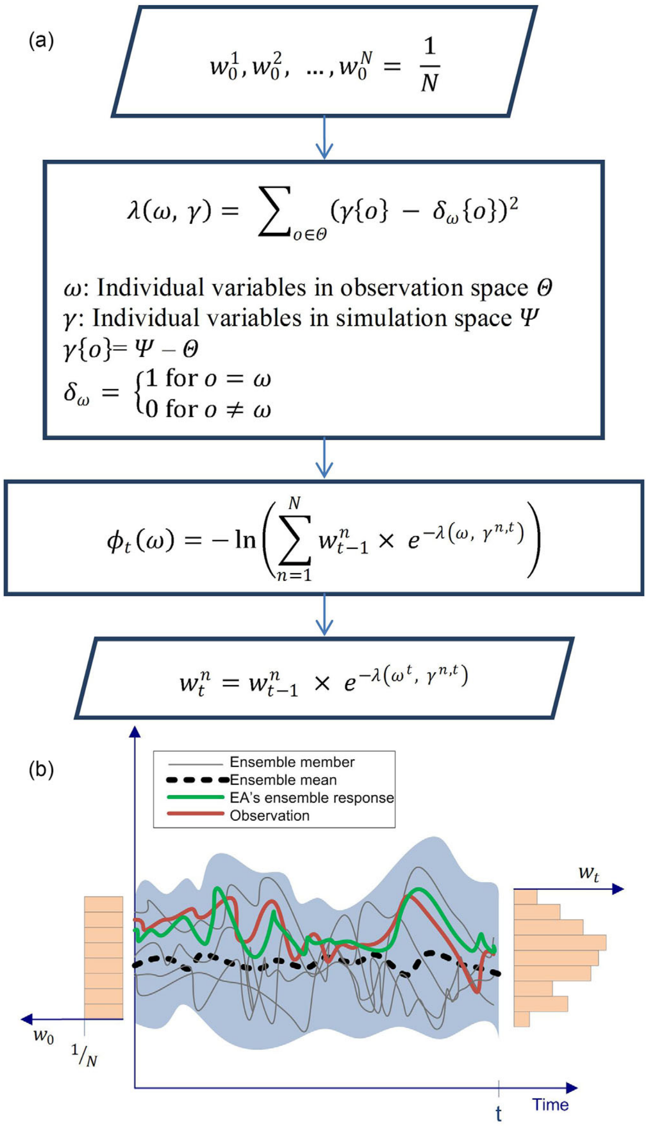

Figure 3. The (a) flowchart and (b) schematic view of the Expert Advice (EA) algorithm.

Previous studies show that averaging the ensemble of multimodel predictions with equal weights does not necessarily lead to the most skillful outcome [*Masson and Knutti*, 2011; *Knutti et al.*, 2010]. In fact, the ensemble mean may be biased by poorly performing models [*Krishnamurti et al.*, 2000] and smooth out the extreme events predictions (Figure 2a). The EA algorithm argues that instead of the ensemble mean, an ensemble response should be selected that is better than each individual ensemble member, plus an error term. The EA algorithm starts with equal weights ($w_0^1, w_0^2, \ldots, w_0^N = \frac{1}{N}$) for all the N ensemble members (including both statistical and dynamical simulations) at the first time step $(t=1)$ of the training period (see Figure 3). In this particular application of the method, there are 11 weights $(i.e., N=11)$ for 11 forecast components at each time step ($\gamma^{n,t}$) (i.e., the 8 dynamical model ensemble means, the NMME grand ensemble mean, and the two statistical predictions). The weight of each member is then updated at each time step based on its relative performance to the others during the past time steps. A loss (error) function, $\lambda(\omega, \gamma)$, is used to adjust the weights of ensemble members based on the observed variable (i.e., ω) and the simulated variable (i.e., γ). The loss function is obtained by optimizing the weight function $\phi_t(\omega)$ as explained in *Vovk* [2001]. Ultimately, the goal of the algorithm is to find the best ensemble response (Figure 3b) with the smallest cumulative error over the training period. More details on EA algorithm is found in *Cheng and AghaKouchak* [2015]. Given the relatively short length of record (1982–2014), we use hindcasts from 1982 up to the last year before the target year (after 2005) for estimating the weights (i.e., training purposes). The model is then validated for the target year based on ground-based observations.

4. Results and Discussion

In this section, we show the results of the proposed hybrid precipitation prediction approach at the spatial resolution of 1° × 1° over the southwest U.S. Precipitation forecasts are presented for different periods during the rainy season of the region; i.e., NDJ, NDJF, NDJFM, DJF, DJFM, and JFM. The results of the statistical precipitation model are also generated for the same forecast periods. This step involves the conditional forecast of precipitation anomaly given the global teleconnection indices, including PDO, MEI, and AMO. The statistical model describes the joint relationship between AMO-MEI (and AMO-PDO) and winter precipitation using copulas (see also equation (4)). These climate indices are averaged over June–October where they show relatively high correlation with the following rainy season precipitation in several regions of the

10.1002/2015WR018547

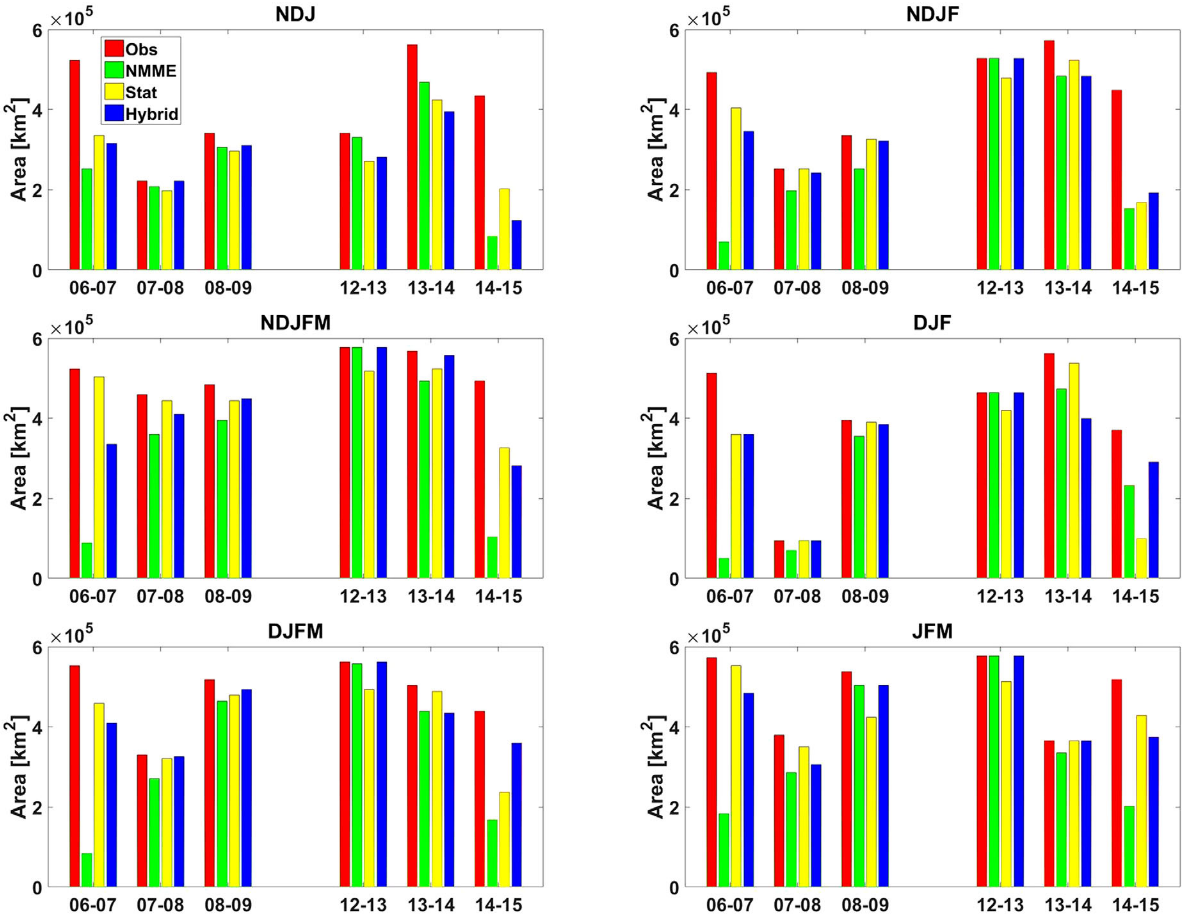

Figure 4. The area (mi^2) with the observed negative precipitation anomaly (light gray bars) correctly captured by the NMME (dark gray bars), statistical model (yellow bars), and hybrid model (blue bars) simulations during 2006–2008 and 2012–2014 droughts. The target prediction periods start at November, December, or January and continues up to the following March.

world [*Schepen et al.*, 2012; *Khedun et al.*, 2014; *Kurtzman and Scanlon*, 2007] including the western U.S. [*Redmond and Koch*, 1991]. It should be noted that there are some sources of uncertainty in reported climate indices such as PDO [*Wen et al.*, 2014] which can influence the relationships between the predictors and precipitation to some extend and consequently affect the statistical model simulations. As explained earlier, the conditional PDF of precipitation was separately estimated for each pair of teleconnection indices (see equation (4)), and the fiftieth percentile (median) is used as the final prediction of associated PDF. The choice of fiftieth percentile from the predictive distribution is another source of uncertainty in statistical model simulations which needs to be studied in future efforts.

The EA algorithm is applied to both statistical model simulations and dynamical model simulations. To evaluate the proposed hybrid framework, we assessed the predictability of the hybrid model and the dynamical model in capturing the negative precipitation anomalies (below-average precipitation) during two major droughts in the past decade; 2006–2008 and 2012–2014. Note that precipitation anomalies for each forecast period at each grid cell are calculated based on the average precipitation over 1982–2014 in that particular grid cell. Figure 4 shows the size of observed area under drought conditions (i.e., negative precipitation anomaly) (light gray bars) and the size of area correctly captured as dry region using the grand ensemble mean of the NMME (dark gray bars), the statistical simulations' mean (yellow bars), and the hybrid framework (blue bars). Note that the size of area is calculated based on the total number of grid cells with observed/simulated negative precipitation anomaly multiplied by the size of each grid cell. As shown, the hybrid model and the statistical model could capture these two drought events better than NMME, especially for the rainy season of 2006–2007 and 2014–2015. The drought predictability for 2014–2015 varies from 28% (NDJ) to 82% (DJFM) for the hybrid model, and 19% (NDJ) to 62% (DJF) for the NMME model.

Overall, for the extreme drought of 2014–2015, the predictability of hybrid model was 10% (NDJ and NDJF) to 50% (DJFM) greater than that of NMME. Similarly, for 2006–2007 drought, the predictability increases by 10% (NDJ) to 60% (NDJF, DJF, and DJFM) after the hybrid-model application. Note that in some other years all the three models could successfully capture drought conditions across the region and their drought predictabilities were rather similar (Figure 4).

Figures 5 and 7 display the spatial distribution of the observed precipitation anomaly (first column), ensemble mean of NMME forecasts (second column), the statistical simulations' mean (third column), and the hybrid simulation (fourth column) during the rainy season of 2006–2007 (Figure 5) and 2014–2015 (Figure 6). The pixels with a positive precipitation anomaly are shown in blue, and those with a negative anomaly are shown in brown. For each target year (e.g., 2006–2007 and 2014–2015), we used the data from 1982 up to the last year before target year to calibrate the hybrid-model parameters, including the weights of the EA algorithm and the copula parameters. This procedure was repeated for each target year at each grid cell ($1° \times 1°$).

As shown in the observations (Figures 4–6), the southwestern U.S. has experienced extreme droughts in 2006–2008 and 2012–2014 periods, specifically in the latter. As shown for 2006–2007 period, the NMME signal was opposite of that of the observations in all the lead times (i.e., NMME indicated wet conditions, but the region experienced a major drought). However, both the statistical model and the hybrid model could capture the 2006–2007 drought much better than NMME. Despite the performance of statistical model, its contribution in the final hybrid model depends on its performance during the entire training period. Likewise, the contribution of the hybrid model depends on its performance during the training period. According to the final weights of statistical and dynamical models (Figure 7), both statistical and dynamical models contribute in the final result of the hybrid model. Although some discrepancies between the hybrid model and the observations are apparent in central California, the overall performance of the hybrid model is better than using solely dynamical or statistical model simulations in capturing the drought of 2006–2007 across the region. In 2014–2015, the NMME could capture the negative anomalies in most parts of California (especially in NDJF and DJF); however, it gives opposite signal for almost entire Nevada. The statistical model, on the other hand, could predict the negative anomalies of the southern part of the region and fails to capture the drought conditions in the northern part. The combination of the two models (i.e., the hybrid model), however, could improve the predictions of the NMME and statistical model for most parts of the region. In addition, the results of Figures 5 and 6 indicate that the hybrid model performs better for relatively long lead times (compare the results of NDJ with other forecast periods).

This study also analyzes the performance of the three models for the wet winter of 2010–2011 (i.e., 2010–2011). Figure 7 compares the predictions of the NMME, statistical model, and the proposed hybrid statistical-dynamical model for the rainy season of 2010–2011. Similar to the previous results, the forecast lead time increases from 3 to 5 months. As shown, the statistical model could not predict the positive anomalies in the region. The grand ensemble mean of NMME forecasts also failed to represent the positive precipitation anomalies (i.e., wet conditions) especially in central and south California. However, the hybrid model slightly improved the predictions for central California and Nevada (Figure 6a). The predictability of wet conditions in 2010–2011 varies from 45% (NDJFM) to 85% (JFM) for the hybrid model and from 35% (NDJ) to 60% (JFM) for the NMME. Overall, the hybrid model improves the predictability (Figure 6b) by 5% (DJFM) to 25% (JFM) relative to the NMME. Comparing the results in Figures 4–6 indicates that all the three models have higher predictability in the selected dry years than in the selected wet year. It should be noted that the wet conditions in 2010–2011 was significantly attributed to a sequence of Atmospheric River (AR) storms [*Zhu and Newell*, 1998]. AR storms are generated by water-vapor streams in the atmosphere and usually supply approximately 20–50% of the annual precipitation and streamflow in California [Dettinger, 2013]. In December 2010, ARs occurred within a week's time and provided half of the average annual precipitation for central and southern California. Although some connections are found between ARs and atmosphere-ocean dynamics such as Madden-Julian Oscillation (MJO) [*Guan et al*., 2012; *Ralph et al*., 2011], North Atlantic Oscillation (NAO) [*Lavers and Villarini*, 2013], Arctic Oscillation (AO), and Pacific North American Index (PNA) [*Guan et al*., 2013], these associations are not yet clearly understood [*Gimeno et al*., 2014], and operate at subseasonal rather than seasonal time scales. Predicting ARs is very challenging, and both dynamical and statistical models have limitations in representing them. This is one of the limitations of the proposed hybrid statistical-dynamical framework and can be improved if the dynamical and statistical

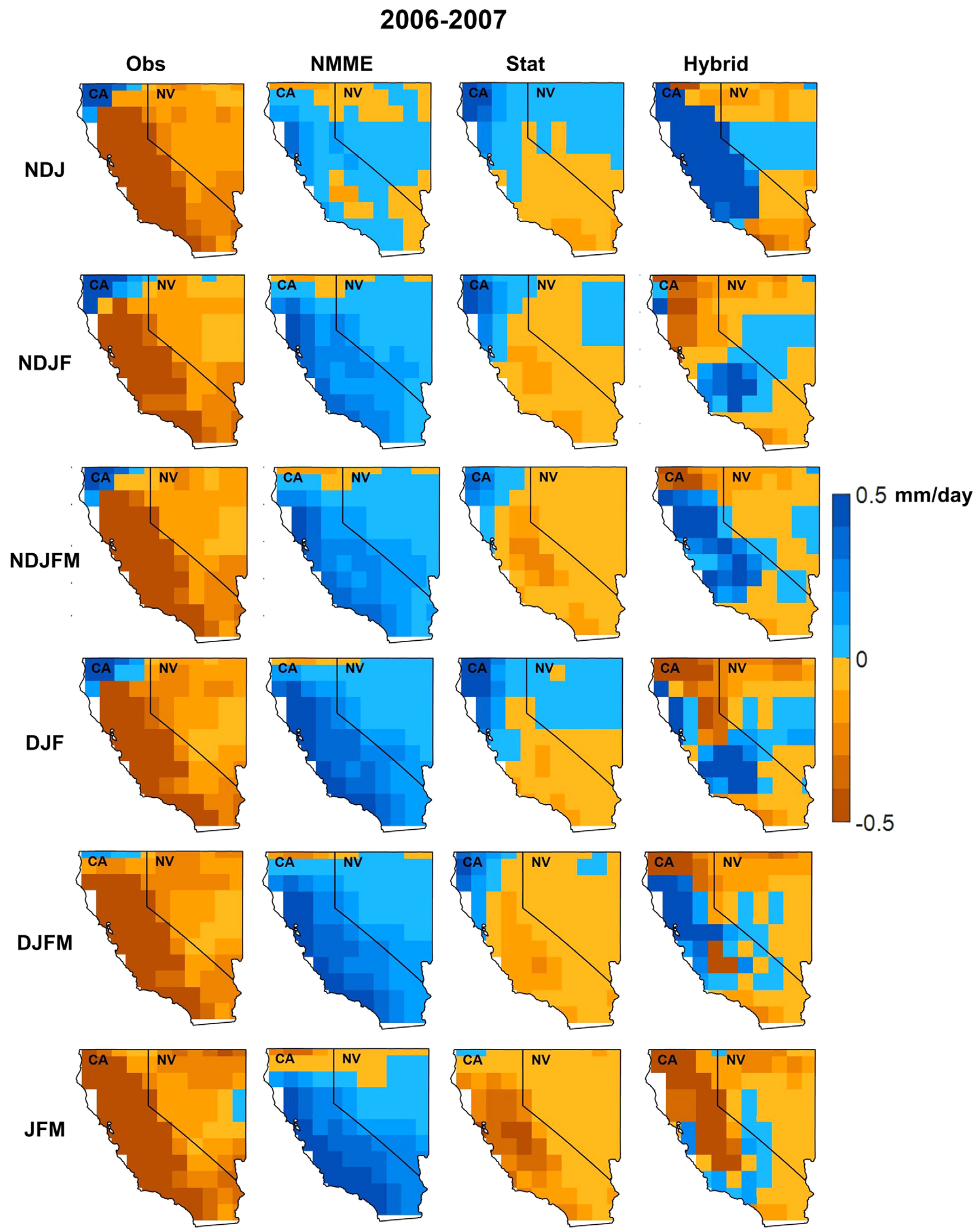

Figure 5. Precipitation anomaly (mm/d) during the rainy season of 2006–2007 with different lead times (NDJ, NDJF, NDJFM, DJF, DJFM, and JFM). Forecasts are initiated from October of each year, i.e., IC = Oct. The (first column) observations, (second column) NMME forecasts, (third column) statistical model predictions, and (fourth column) hybrid model predictions are shown for the target periods of each year.

models provide more accurate simulations of the ARs, or if other teleconnection indices are discovered that more strongly reflect a tendency for ARs within a given season.

Insight into the contributions of the different components of the hybrid framework can be gained from assessing the weights obtained for the statistical and dynamical forecasts, for different seasonal predictands. Figure 8 displays the spatial distribution of weights obtained from the EA algorithm for the grand ensemble mean of the NMME and the statistical model simulations. As seen, the ensemble mean of the NMME attained generally larger weights in northern California relative to the statistical model simulations. In contrast, the statistical model simulations obtained larger weights in southern California and central to

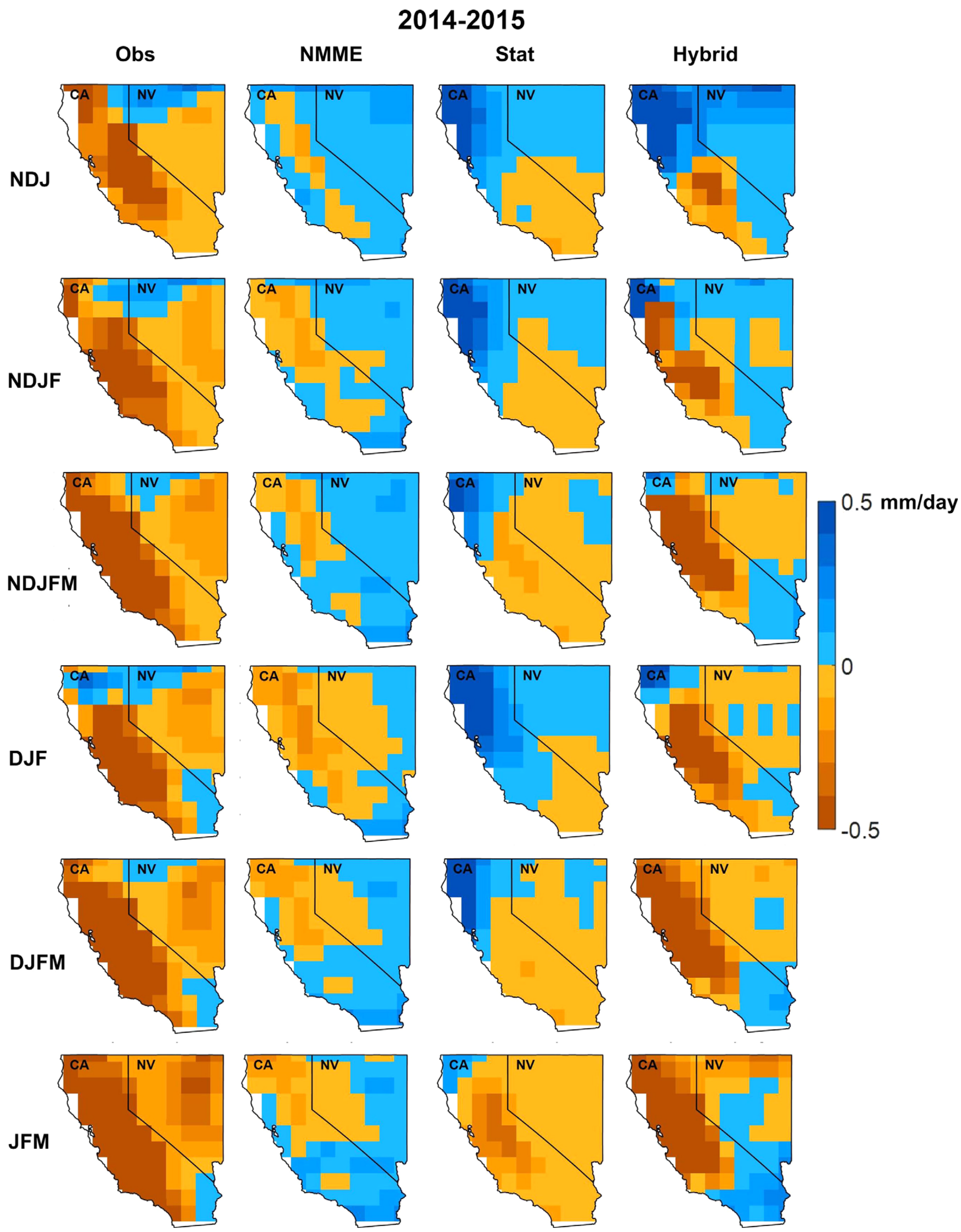

Figure 6. Precipitation anomaly (mm/d) during the rainy season of 2014–2015 with different lead times (NDJ, NDJF, NDJFM, DJF, DJFM, and JFM). Forecasts are initiated from October of each year, i.e., IC = October. The (first column) observations, (second column) NMME forecasts, (third column) statistical model predictions, and (fourth column) hybrid model predictions are shown for the target periods of each year.

southern Nevada. Neither model, however, receives large weights in central California and northern Nevada, which means that the rest of ensemble members (corresponding to the ensemble mean of each of the eight NMME models) in the hybrid model ensemble are given large weights for those regions.

5. Concluding Remarks

In recent decades, drought monitoring has improved significantly due to a range of satellite observations and hydroclimate reanalysis data sets [*Xia et al.*, 2012]. However, drought prediction at seasonal to

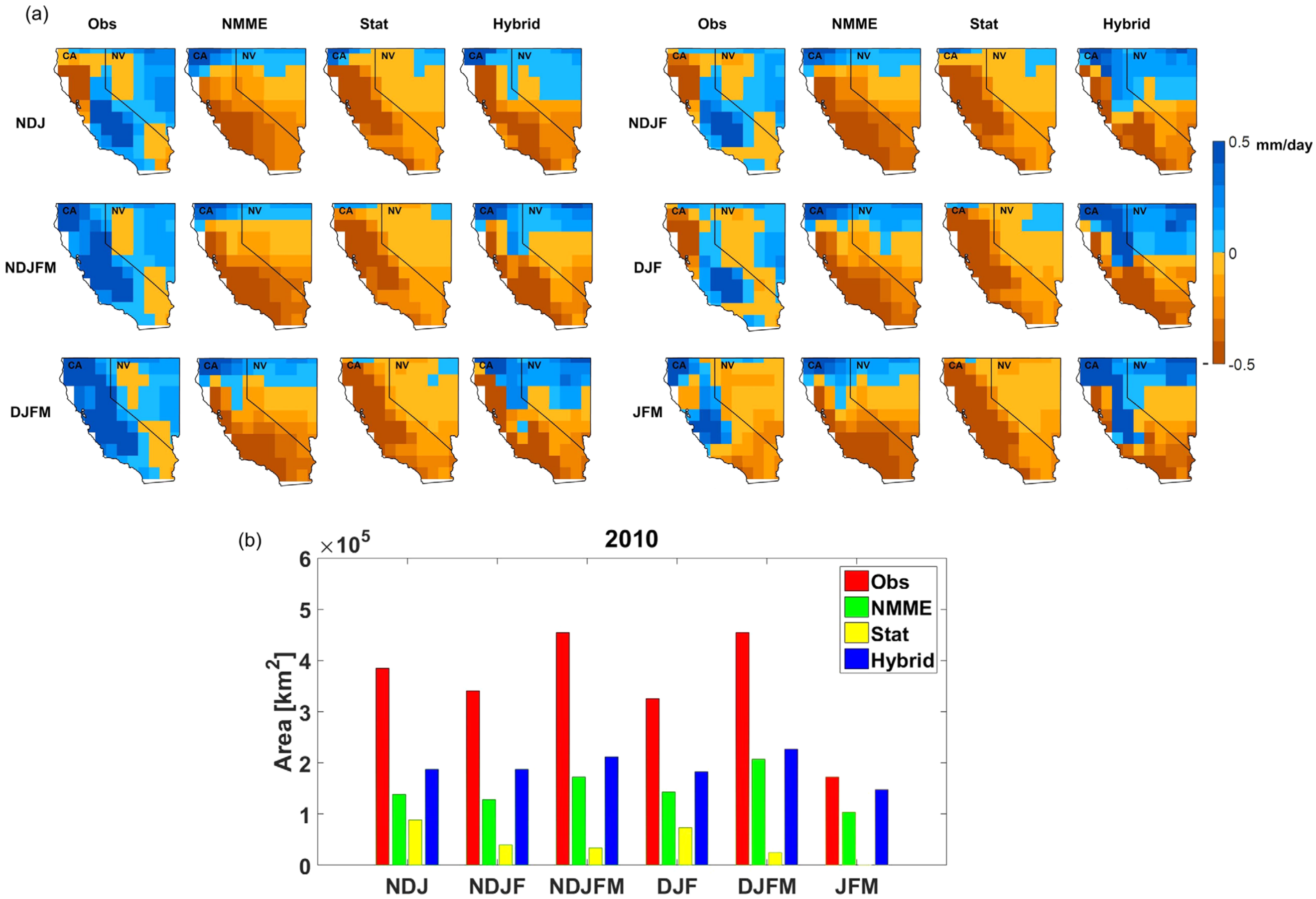

Figure 7. Comparing the performance of hybrid model and the dynamical and statistical models in (a) capturing the wet conditions and (b) predictability of positive anomalies during the rainy season of 2010–2011.

inter-annual scales remains a grand challenge at a regional scale, as evidenced by forecasts during the recent drought in the western U.S. [*Seager et al*., 2014]. A breakthrough in predicting precipitation can lead to major improvements in water management and risk reduction. This study presents a hybrid seasonal climate forecasting approach that combines physically based dynamical models and statistical

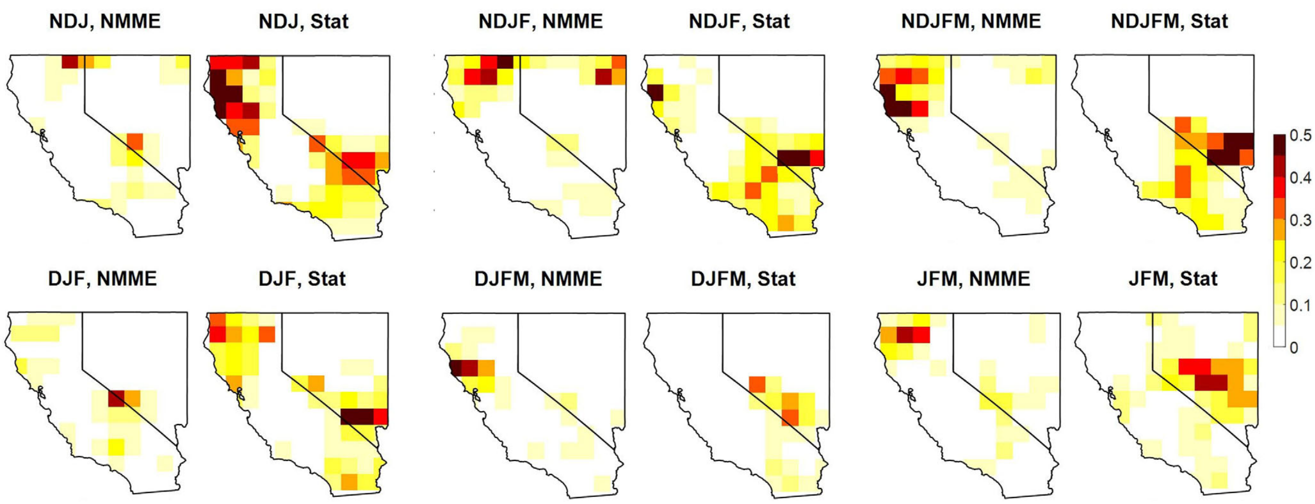

Figure 8. Weight distribution obtained from the EA algorithm for (left) the NMME simulations and (right) the statistical model simulations for different prediction periods (i.e., NDJ, NDJF, NDJFM, DJF, DJFM, and JFM).

models, and investigates its potential for improving drought prediction in the southwestern U.S. The proposed hybrid model combines dynamical model forecasts from the NMME with Bayesian statistical forecasts using teleconnections indices (PDO, MEI, and AMO). The hybrid model utilizes the EA algorithm to merge the dynamical model forecasts and statistical model predictions. The hybrid method aims to improve drought prediction by combining these two fundamentally different seasonal precipitation prediction methods.

The results indicate that although the dynamical model simulations capture some of the recent droughts, they do not offer high predictability, corroborating prior assessments of dynamical model precipitation prediction skill. The integration of the statistical and dynamical methods, however, appears to improve the prediction of seasonal precipitation in this case study. The predictability of seasonal precipitation increases by 5–60% after the application of hybrid model. Overall, the hybrid framework performs better in predicting below-normal precipitation than above-normal precipitation (Figures 4–7). While there are still major challenges for reliable seasonal drought predictions, the results of this study encourage further exploration of hybrid dynamical-statistical methods in different regions with different climate regimes. We acknowledge that several issues such as the relatively short record, uncertainty in the observed dependencies, and model parameterization may have affected predictions of wet and drought anomalies. More efforts and evaluations of the proposed model are required before this model can be used in water resources management.

Drought prediction studies often focus on national or continental-scale predictions with less attention to their adequacy for regional conditions and impacts. The manifestation of drought impacts at very local to regional scales, however, motivates interest in evaluating drought-related prediction approaches at local to regional scales. At regional scales, different sources of predictability may be harnessed through different forecasting methods. For instance, the strength of climate indices (e.g., ENSO) influence on local climate varies in different regions and seasons, and dynamical climate forecasting model performance varies similarly. Here the hybrid model is applied for the southwestern U.S. by including climatic indicators that have been shown to affect precipitation in this region. This modeling framework can potentially be applied to other regions by integrating the relevant region-specific climatic indicators, as well as the NMME predictions that have a global extent.

Appendix A

Pacific Decadal Oscillation (PDO). The Pacific Decadal Oscillation (PDO) indicates the long-term variability in monthly SST anomalies over the North Pacific Ocean [*Mantua et al*., 1997]. Precipitation pattern in the western U.S. is rather correlated with the PDO phase; where in the southwest U.S., drought frequency tends to increase in the cool (negative) phase of PDO [*McCabe et al*., 2004]. It has been also evidenced that PDO augments the impacts of ENSO [*McCabe and Dettinger*, 1999] and AMO [*McCabe et al*., 2004] on the climate variability of the western U.S.

Multivariate ENSO Index (MEI). The El Nino-Southern Oscillation (ENSO) is an important coupled ocean-atmosphere phenomenon with a strong impact on interannual climate variability. The Multivariate ENSO Index (MEI) [*Wolter and Timlin*, 1998] is a comprehensive index consisting of multiple meteorological components for monitoring ENSO events. It combines six main observed variables over the tropical Pacific: the sea level pressure, zonal and meridional components of the surface wind, sea surface temperature, surface air temperature, and the total cloudiness fraction of the sky. The MEI is defined as the first unrotated principal component (PC) [*Jolliffe*, 2002] of the above mentioned six variables, which are collected from the International Comprehensive Ocean-Atmosphere Data Set (ICOADS) at NOAA.

Atlantic Multidecadal Oscillation (AMO). The Atlantic Multidecadal Oscillation (AMO) influences the air temperature and precipitation over the Northern Hemisphere, particularly North America and Europe. It reflects the long-term changes in the sea surface temperature of the North Atlantic Ocean, whereas the cool and warm phases may last for 20–40 years. Drought frequency over North America is associated with AMO phases [*McCabe et al*., 2004]. The positive phase of the AMO often leads to droughts in the southwest and midwest U.S. and results in above-average precipitation in the Pacific Northwest and Florida. The impact is opposite during the negative phase of the AMO.

Acknowledgments

This study is partially supported by National Aeronautics and Space Administration (NASA) award NNX15AC27G and National Oceanic and Atmospheric Administration (NOAA) award NA14OAR4310222. We also acknowledge the discussions and feedback we have received from Jeanine Jones and Michael Anderson from the California Department of Water Resources (DWR). Supplemental funding (award 4600010378 TASK ORDER UCOP2_5) from DWR to develop the proposed analog-year model is also greatly acknowledged. We also thank Soroosh Sorooshian and Kenneth Mitchell for providing constructive comments on an earlier draft of this manuscript. The authors appreciate the thoughtful comments and suggestions from three anonymous reviewers and the Associate Editor that led to substantial improvements in the revised version. The monthly records of teleconnection indices are obtained from the Earth System Research Laboratory at the National Oceanic and Atmospheric Administration (NOAA) (http://www.esrl.noaa.gov/psd/data/climateindices/list/). Retrospective NMME simulations for January 1982 to December 2010 are available at the International Research Institute for Climate and Society (IRI)'s climate data library.

References

AghaKouchak, A., L. Cheng, O. Mazdiyasni, and A. Farahmand (2014), Global warming and changes in risk of concurrent climate extremes: Insights from the 2014 California drought, *Geophys. Res. Lett.*, *41*, 8847–8852, doi:10.1002/2014GL062308.

AghaKouchak, A., D. Feldman, M. Hoerling, T. Huxman, and J. Lund (2015), Recognize Anthropogenic Drought, *Nature*, *524*(7566), 409–4011, doi:10.1038/524409a.

Bougeault, P., et al. (2010), The THORPEX Interactive Grand Global Ensemble, *Bull. Am. Meteorol. Soc.*, *91*, 1059–1072.

Becker, E., H. van den Dool, and Q. Zhang (2014), Predictability and Forecast Skill in NMME, *J. Clim.*, *27*, 5891–5906.

Bradley, R. S., H. F. Diaz, G. N. Kiladis, and J. K. Eischied (1987), ENSO signal in continental temperature and precipitation records, *Nature*, *327*, 497–501.

Buser, C. M., H. R. Künsch, and C. Schär (2010), Bayesian multi-model projections of climate: Generalization and application to ENSEMBLES results, *Clim. Res.*, *44*, 227–241.

Cayan, D. R., M. D. Dettinger, H. F. Diaz, and N. E. Graham (1998), Decadal variability of precipitation over western North America, *J. Clim.*, *11*(12), 3148–3166.

Cayan, D. R., T. Das, D. W. Pierce, T. P. Barnett, M. Tyree, and A. Gershunov (2010), Future dryness in the southwest US and the hydrology of the early 21st century drought, *Proc. Natl. Acad. Sci. U. S. A.*, *107*, 21,271–21,276.

Cheng, L., and A. AghaKouchak (2015), A methodology for deriving ensemble response from multimodel simulations, *J. Hydrol.*, *522*, 49–57, doi:10.1016/j.jhydrol.2014.12.025.

Cheng, L., et al. (2016), How has human-induced climate change affected California Drought Risk?, *J. Clim.*, *29*, 111–120.

Coelho, C. A. S., S. Pezzulli, M. Balmaseda, F. J. Doblas-Reyes, and D. B. Stephenson (2004), Forecast calibration and combination: A simple Bayesian approach for ENSO, *J. Clim.*, *17*, 1504–1516.

Cohen, J., and J. Jones (2011), A new index for more accurate winter predictions, *Geophys. Res. Lett.*, *38*, L21701, doi:10.1029/2011GL049626.

Cook, B. I., T. R. Ault, and J. E. Smerdon (2015), Unprecedented 21st century drought risk in the American Southwest and Central Plains, *Sci. Adv.*, *1*(1), e1400082.

DeFlorio, M. J., D. W. Pierce, D. R. Cayan, and A. J. Miller (2013), Western U.S. extreme precipitation events and their relation to ENSO and PDO in CCSM4, *J. Clim.*, *26*, 4231–4243.

Dettinger, M. D. (2013), Atmospheric rivers as drought busters on the U.S. West Coast, *J. Hydrometeorol.*, *14*, 1721–1732.

Diaz, H. F., and G. N. Kiladis (1992), Atmospheric teleconnections associated with the extreme phase of the Southern Oscillation, in *El Nino: Historical and Paleoclimatic Aspects of the Southern Oscillation*, edited by H. F. Diaz and V. Markgraf, pp. 7–28, Cambridge Univ. Press, Cambridge, U. K.

Dupuis, D. J. (2007), Using copulas in hydrology: Benefits, cautions, and issues, *J. Hydrol. Eng.*, *12*(4), 381–393.

Favre, A. C., S. E. Adlouni, L. Perreault, N. Thiéonge, and B. Bobée (2004), Multivariate hydrological frequency analysis using copulas, *Water Resour. Res.*, *40*, W01101, doi:10.1029/2003WR002456.

Folland, C., J. Owen, M. N. Ward, and A. Colman (1991), Prediction of seasonal rainfall in the Sahel region using empirical and dynamical methods, *J. Forecasting*, *10*(1–2), 21–56.

Gao, H., Y. G. Wang, and J. H. He (2006), Weakening significance of ENSO as a predictor of summer precipitation in China, *Geophys. Res. Lett.*, *33*, L09807, doi:10.1029/2005GL025511.

Gershunov, A. (1998), ENSO influence on intraseasonal extreme rainfall and temperature frequencies in the contiguous United States: Implications for long-range predictability, *J. Clim.*, *11*, 3192–3203.

Gimeno, L., R. Nieto, M. Vázquez, and D. A. Lavers (2014), Atmospheric rivers: A mini-review, *Front. Earth Sci.*, *2*, 2, doi:10.3389/feart.2014.00002.

Guan, B., D. E. Waliser, N. P. Molotch, E. J. Fetzer, and P. J. Neiman (2012), Does the Madden–Julian oscillation influence wintertime atmospheric rivers and Snowpack in the Sierra Nevada?, *Mon. Weather Rev.*, *140*, 325–342.

Guan, B., N. P. Molotch, D. E. Waliser, E. J. Fetzer, and P. J. Neiman (2013), The 2010/2011 snow season in California's Sierra Nevada: Role of atmospheric rivers and modes of large-scale variability, *Water Resour. Res.*, *49*, 6731–6743, doi:10.1002/wrcr.20537.

Hao, Z., and A. AghaKouchak (2013), Multivariate standardized drought index: A parametric multi-index model, *Adv. Water Resour.*, *57*, 12–18, doi:10.1016/j.advwatres.2013.03.009.

Hartmann, H., S. Becker, and L. King (2008), Predicting summer rainfall in the Yangtze River basin with neural networks, *Int. J. Climatol.*, *28*, 925–936.

Hewitt, C. D. (2004), Ensembles-based predictions of climate changes and their impacts, *Eos Trans. AGU*, *85*(52), 566–566.

Hidalgo, H. G., and J. A. Dracup (2003), El ENSO and PDO effects on hydroclimatic variations of the Upper Colorado River Basin, *J. Hydrometeorol.*, *4*(1), 5–23.

Hoerling, M. P., A. Kumar, and M. Zhong (1997), El Niño, La Niña, and the Nonlinearity of Their Teleconnections, *J. Clim.*, *10*, 1769–1786.

Infanti, J. M., and B. P. Kirtman (2015), North American rainfall and temperature prediction response to the diversity of ENSO, *Clim. Dyn.*, *46*, 3007–3023.

Jia, L., et al. (2015), Improved seasonal prediction of temperature and precipitation over land in a high-resolution GFDL Climate Model, *J. Clim.*, *28*, 2044–2062.

Joe, H. (1997), *Multivariate Models and Dependence Concepts*, Chapman and Hall, London, U. K.

Jolliffe, I. (2002), *Principal component analysis*, John Wiley & Sons, Ltd.

Keeley, J. E., H. Safford, C. J. Fotheringham, J. Franklin, and M. Moritz (2009), The 2007 southern California wildfires: Lessons in complexity, *J. For.*, *107*(6), 287–296.

Kelly, K. S., and R. Krzysztofowicz (1997), A bivariate meta-Gaussian density for use in hydrology, *Stochastic Hydrol. Hydraul.*, *11*(1), 17–31.

Khedun, C. P., A. K. Mishra, V. P. Singh, and J. R. Giardino (2014), A copula-based precipitation forecasting model: Investigating the interdecadal modulation of ENSO's impacts on monthly precipitation, *Water Resour. Res.*, *50*, 580–600, doi:10.1002/2013WR013763.

Kiladis, G. N., and H. F. Diaz (1989), Global climate anomalies associated with extremes of the Southern Oscillation, *J. Clim.*, *2*, 1069–1090.

Kim, H. M., P. J. Webster, and J. A. Curry (2012), Seasonal prediction skill of ECMWF System 4 and NCEP CFSv2 retrospective forecast for the Northern Hemisphere Winter, *Clim. Dyn.*, *39*(12), 2957–2973.

Kirtman, B. P., et al. (2014), The North American multimodel ensemble: Phase-1 seasonal-to-interannual prediction; Phase-2 toward developing intraseasonal prediction, *Bull. Am. Meteorol. Soc.*, *95*, 585–601.

Knutti, R., R. Furrer, C. Tebaldi, J. Cermak, and G. A. Meehl (2010), Challenges in combining projections from multiple climate models, *J. Clim.*, *23*(10), 2739–2758.

Krishnamurti, T., C. Kishtawal, Z. Zhang, T. LaRow, D. Bachiochi, E. Williford, S. Gadgil, and S. Surendran (2000), Multimodel ensemble forecasts for weather and seasonal climate, *J. Clim.*, *13*(23), 4196–4216.

Kumar, A., J. Bhaskar, Q. Zhang, and L. Bounoua (2007), A new methodology for estimating the unpredictable component of seasonal atmospheric variability, *J. Clim.*, *20*, 3888–3901.

Kurtzman, D., and B. R. Scanlon (2007), El Nino-Southern Oscillation and Pacific Decadal Oscillation impacts on precipitation in the southern and central United States: Evaluation of spatial distribution and predictions, *Water Resour. Res.*, *43*, W10427, doi:10.1029/2007WR005863.

Lavers, D. A., and G. Villarini (2013), The nexus between atmospheric rivers and extreme precipitation across Europe, *Geophys. Res. Lett.*, *40*, 3259–3264, doi:10.1002/grl.50636.

Luo, L., E. F. Wood, and M. Pan (2007), Bayesian merging of multiple climate model forecasts for seasonal hydrological predictions, *J. Geophys. Res.*, *112*, D10102, doi:10.1029/2006JD007655.

Ma, F., A. Ye, X. Deng, Z. Zhou, X. Liu, Q. Duan, J. Xu, C. Miao, Z. Di, and W. Gong (2015), Evaluating the skill of NMME seasonal precipitation ensemble predictions for 17 hydroclimatic regions in continental China, *Int. J. Climatol.*, *36*, 132–144, doi:10.1002/joc.4333.

Madadgar, S., and H. Moradkhani (2013), A Bayesian framework for probabilistic seasonal drought forecasting, *J. Hydrometeorol.*, *14*, 1685–1705.

Madadgar, S., and H. Moradkhani (2015), Improved Bayesian multimodeling: Integration of copulas and Bayesian model averaging, *Water Resour. Res.*, *50*, 9586–9603, doi:10.1002/2014WR015965.

Mantua, N. J., S. R. Hare, Y. Zhang, J. M. Wallace, and R. C. Francis (1997), A Pacific interdecadal climate oscillation with impacts on salmon production, *Bull. Am. Meteorol. Soc.*, *78*(6), 1069–1079.

Masson, D., and R. Knutti (2011), Climate model genealogy, *Geophys. Res. Lett.*, *38*, L08703, doi:10.1029/2011GL046864.

McCabe, G. J., and M. D. Dettinger (1999), Decadal variations in the strength of ENSO teleconnections with precipitation in the western United States, *Int. J. Climatol.*, *19*(13), 1399–1410.

McCabe, G. J., M. A. Palecki, and J. L. Betancourt (2004), Pacific and Atlantic Ocean influences on multidecadal drought frequency in the United States, *Proc. Natl. Acad. Sci. U. S. A.*, *101*(12), 4136–4141.

Merryfield, W. J., W. S. Lee, G. J. Boer, V. V. Kharin, J. F. Scinocca, G. M. Flato, R. S. Ajayamohan, J. C. Fyfe, Y. Tang, and S. Polavarapu (2013), The Canadian seasonal to interannual prediction system. Part I: Models and initialization, *Mon. Weather Rev.*,*141*, 2910–2945.

Najafi, M. R., and H. Moradkhani (2015), Ensemble combination of seasonal streamflow forecasts, *J. Hydrol. Eng.*, *21*(1), 04015043.

Nelsen, R. B. (1999), *An Introduction to Copulas*, Springer, N. Y.

Obled, C., G. Bontron, and R. Garçon (2002), Quantitative precipitation forecasts: A statistical adaptation of model outputs through an analogues sorting approach, *Atmos. Res.*, *63*(3), 303–324.

Palmer, T. N., et al. (2004), Development of a European multimodel ensemble system for seasonal-to-interannual prediction (DEMETER), *Bull. Am. Meteorol. Soc.*, *85*(6), 853–872.

Peng, Z., Q. J. Wang, J. C. Bennett, P. Pokhrel, and Z. Wang (2014), Seasonal precipitation forecasts over China using monthly large-scale oceanic-atmospheric indices, *J. Hydrol.*, *519*, 792–802.

Raftery, A. E., T. Gneiting, F. Balabdaoui, and M. Polakowski (2005), Using Bayesian model averaging to calibrate forecast ensembles, *Mon. Weather Rev.*, *133*, 1155–1174.

Rajeevan, M., D. S. Pai, R. A. Kumar, and B. Lal (2007), New statistical models for long-range forecasting of southwest monsoon rainfall over India, *Clim. Dyn.*, *28*(7-8), 813–828.

Ralph, F. M., P. J. Neiman, G. N. Kiladis, K. Weickmann, and D. W. Reynolds (2011), A multiscale observational case study of a Pacific atmospheric river exhibiting tropical–extratropical connections and a mesoscale frontal wave, *Mon. Weather Rev.*, *139*, 1169–1189.

Rasmusson, E. M., and J. M. Wallace (1983), Meteorological aspects of the El Nino/Southern Oscillation, *Science*, *222*, 1195–1202.

Redmond, K. T., and R. W. Koch (1991), Surface climate and streamflow variability in the western United States and their relationship to largescale circulation indexes, *Water Resour. Res.*, *27*, 2381–2399.

Ropelewski, C. F., and M. S. Halpert (1986), North American precipitation and temperature patterns associated with the El Nino/Southern Oscillation (ENSO), *Mon. Weather Rev.*, *114*(12), 2352–2362.

Saha, S., et al. (2014), The NCEP Climate Forecast System Version 2, *J. Clim.*, *27*, 2185–2208.

Savtchenko, A. K., G. Huffman, and B. Vollmer (2015), Assessment of precipitation anomalies in California using TRMM and MERRA data, *J. Geophys. Res. Atmos.*, *120*, 8206–8215, doi:10.1002/2015JD023573.

Schepen, A., and Q. J. Wang (2013), Towards accurate and reliable forecasts of Australian seasonal rainfall by calibrating and merging multiple coupled GCMs, *Mon. Weather Rev.*, *141*, 4554–4563.

Schepen, A., Q. J. Wang, and D. Robertson (2012), Evidence for using lagged climate indices to forecast Australian seasonal rainfall, *J. Clim.*, *25*, 1230–1246.

Schepen, A., Q. J. Wang, and D. E. Robertson (2014), Seasonal forecasts of Australian rainfall through calibration and bridging of coupled GCM outputs, *Mon. Weather Rev.*, *142*, 1758–1770.

Seager, R., Y. Kushnir, C. Herweijer, N. Naik, and J. Velez (2005), Modeling of tropical forcing of persistent droughts and pluvials over western North America: 1856–2000, *J. Clim.*, *18*, 4065–4088.

Seager, R., et al. (2007), Model projections of an imminent transition to a more arid climate in southwestern North America, *Science*, *316*(5828), 1181–1184.

Seager, R., M. Hoerling, S. Schubert, H. Wang, B. Lyon, A. Kumar, J. Nakamura, and N. H. Henderson (2014), Causes and predictability of the 2011-14 California Drought, assessment report, NOAA Modeling, Analysis, Predictions and Projections Program (MAPP), National Integrated Drought Information System (NIDIS). [Available at http://hdl.handle.net/10590/2762.]

Sharma, A. (2000), Seasonal to interannual rainfall probabilistic forecasts for improved water supply management: Part 3—A nonparametric probabilistic forecast model, *J. Hydrol.*, *239*(1–4), 249–258.

Shukla, S., A. Steinemann, S. F. Iacobellis, and D. R. Cayan (2015a), Annual drought in California: Association with monthly precipitation and climate phases, *J. Appl. Meteorol. Climatol.*, *54*(11), 2273–2281.

Shukla, S., et al. (2015b), Temperature impacts on the water year 2014 drought in California, *Geophys. Res. Lett.*, *42*, 4384–4393, doi:10.1002/2015GL063666.

Tang, Q., A. W. Wood, and D. P. Lettenmaier (2009), Real-time precipitation estimation based on index station percentiles, *J. Hydrometeorol.*, *10*, 266–277.

Trenberth, K. E. (1984), Signal versus noise in the Southern Oscillation, *Mon. Weather Rev.*, *112*(2), 326–332.

Trenberth, K. E. (1997), The definition of El Nino, *Bull. Am. Meteorol. Soc.*, *78*, 2771–2777.

Vovk, V. (2001), Competitive on-line statistics, *Int. Stat. Rev.*, *69*(2), 213–248.

Wang, B., et al (2009), Advance and prospectus of seasonal prediction: Assessment of the APCC/CliPAS 14-model ensemble retrospective seasonal prediction (1980–2004), *Clim. Dyn.*, *33*(1), 93–117.

Weigel, A. P., M. A. Liniger, and C. Appenzeller (2008), Can multi-model combination really enhance the prediction skill of probabilistic ensemble forecasts?, *Q. J. R. Meteorol. Soc.*, *134*, 241–260, doi:10.1002/qj.210.

Weigel, A. P., R. Knutti, M. A. Liniger, and C. Appenzeller (2010), Risks of model weighting in multimodel climate projections, *J. Clim.*, *23*, 4175–4191.

Wen, C., A. Kumar, and Y. Xue (2014), Factors contributing to uncertainty in Pacific Decadal Oscillation index, *Geophys. Res. Lett.*, *41*, 7980–7986, doi:10.1002/2014GL061992.

Westerling, A. L., A. Gershunov, T. J. Brown, D. R. Cayan, and M. D. Dettinger (2003), Climate and wildfire in the Western United States, *Bull. Am. Meteorol. Soc.*, *84*, 595–604.

Wolter, K., and M. S. Timlin (1998), Measuring the strength of ENSO events: how does 1997/98 rank?, *Weather*, *53*(9), 315–324.

Wood, A. W. (2008), The University of Washington Surface Water Monitor: An experimental platform for national hydrologic assessment and prediction, in *Proceedings of the American Meteorological Society (AMS) 22nd Conference on Hydrology*, New Orleans, Louisiana, USA, January 20-24, 2008, 13 pp.

Woodhouse, C. A., D. M. Meko, G. M. MacDonald, D. W. Stahle, and E. R. Cook (2010), A 1,200-year perspective of 21st century drought in southwestern North America, Proc. *Natl. Acad. Sci.*, *107*(50), 21,283–21,288.

Wu, Z. W., B. Wang, J. P. Li, and F. F. Jin (2009), An empirical seasonal prediction model of the East Asian summer monsoon using ENSO and NAO, *J. Geophys. Res.*, *114*, D18120, doi:10.1029/2009JD011733.

Xia, Y., et al. (2012), Continental-scale water and energy flux analysis and validation for the North American Land Data Assimilation System project phase 2 (NLDAS-2): 1. Intercomparison and application of model products, *J. Geophys. Res.*, *117*, D03109, doi:10.1029/2011JD016048.

Yang, S., Y. Jiang, D. Zheng, R. W. Higgins, Q. Zhang, V. E. Kousky, and M. Wen (2009), Variations of U.S. regional precipitation and simulations by the NCEP CFS: Focus on the southwest, *J. Clim.*, *22*, 3211–3231.

Yue, S., T. B.M. J. Ouarda, and B. Bobée (2001), A review of bivariate gamma distributions for hydrological application, *J. Hydrol.*, *246*(1–4), 1–18.

Zhang, S., M. J. Harrison, A. Rosati, and A. T. Wittenberg (2007), System design and evaluation of coupled ensemble data assimilation for global oceanic climate studies, *Mon. Weather Rev.*, *135*, 3541–3564, doi:10.1175/MWR3466.1.

Zhu, Y., and R. E. Newell (1998), A proposed algorithm for moisture fluxes from atmospheric rivers, *Mon. Weather Rev.*, *126*, 725–735.